# Infrared Spectra and Density Functional Theory Calculations of Group 8 Transition Metal Sulfide Molecules

**Binyong Liang, Xuefeng Wang, and Lester Andrews***

*Department of Chemistry, University of Virginia, P.O. Box 400319, Charlottesville, Virginia 22904-4319*

*Received: February 3, 2009; Revised Manuscript Received: February 26, 2009*

Small sulfur molecules were reacted with laser-ablated Fe, Ru, and Os atoms in excess argon and condensed at 7 K. Reaction products were identified from matrix infrared spectra through sulfur-34 isotopic shifts, spectra of sulfur isotopic mixtures, and frequencies from density functional calculations. The strongest absorptions of the $MS_2$ disulfide molecules are observed at 540.2, 535.5, and 537.5 $cm^{-1}$, respectively, for the group 8 metals, and a 523.2 $cm^{-1}$ band is assigned to the FeS vibrational fundamental in solid argon. The $FeS_2^-$ anion was detected in the spectrum at 542.1 $cm^{-1}$. The $RuS_2$ absorption exhibited resolved natural ruthenium isotopic splittings. Evidence is also presented for side-bound $M(S_2)$ isomers and $MS_4$ molecules with different structures including $Fe(S_2)_2$, $(S_2)RuS_2$, and tetrahedral $OsS_4$. Although $OsO_4$ is a well-known molecule, this, we believe, is the first experimental observation of $OsS_4$.

## Introduction

Transition metal sulfides have attracted considerable attention because of their widely recognized importance in many biological and industrial processes.[1] In particular, iron sulfides have generated the most interest, and iron pyrite, $FeS_2$, has a textbook structure.[2,3] Iron sulfides are relevant to the origin of life on Earth,[4,5] and they are also cited as evidence for ancient life on extraterrestrial samples.[6] In biological systems, iron−sulfur clusters are not only involved in electron transfer and organic radical generations but also serve as immediate sulfur donors in various processes.[7−9] In industrial applications, bulk transition metal sulfides are commonly employed as catalysts for hydrodesulfurization. Ruthenium sulfide clusters have been extensively studied, in part, because bulk $RuS_2$ is among the most active catalysts for binary metal sulfides.[10−12] In addition, reports have also shown that osmium sulfides play important roles in volcanic studies.[13]

On the molecular level, group 8 transition metal sulfides have been investigated less, and most research has focused on the ionic iron sulfides. A Fourier tranform mass spectrometry study reported the formation of $FeS_n^+$ ($n = 1-6$) in the sequential reactions of $Fe^+$ with ethylene sulfide, and photodissociation and ion−molecule reactions provided various bond energies.[14] Photoelectron spectroscopy of ion−sulfur cluster anions has been reported. In the case of $FeS^-$, the energy differences between three excited electronic states and the ground state of FeS were determined,[15] and a higher resolution study found a $520 \pm 30$ $cm^{-1}$ vibrational spacing for FeS and measured electron affinities for $FeS_n$ ($n = 1-6$) species.[16] Using mass-spectrometric techniques and complementary ab initio and density functional theory calculations, structural and thermodynamic aspects of $FeS^+$ and $FeS_2^+$ in the gas phase have been determined.[17,18] By means of two successive collision-induced electron detachments from $FeS^-$, the ionization energy of FeS has also been determined.[17] A recent photodissociation spectroscopic study of $FeS^+$ observed the vibrational frequency for the excited $^6\Pi$ state.[19] An earlier matrix isolation work assigned a band at 542 $cm^{-1}$ to the FeS fundamental in the argon matrix,[20] and a recent microwave spectrum of FeS provided a basis for estimation of the fundamental frequency (506 $cm^{-1}$) from centrifugal distortion constants.[21] Theoretical calculations have determined the $^5\Delta$ ground state for FeS depending on the method employed.[22−25] Recent DFT calculations compared cyclic $Fe(S_2)$ and $FeS_2$ and found bent $FeS_2$ to be 0.18 eV lower in energy.[18] To the best of our knowledge, there has been no investigation of ruthenium and osmium sulfide molecules so the present report will make an initial contribution.

Comparison of metal oxide and sulfide molecules formed with the different metals in a transition metal series or group is of chemical interest, but there have been many fewer investigations of molecular sulfides.[21,22] Recent Fe atom reactions with $O_2$ found FeO, the bent OFeO dioxide, and side-bound dioxygen complexes $Fe(O_2)$ as major products.[26] Later reactions with laser-ablated Ru and Os atoms provided the $MO_2$ dioxide molecules as major products, and the $MO_3$ and $MO_4$ molecules were formed on sample annealing.[27]

Previous reactions of group 4 and 5 transition metals with small sulfur molecules gave mostly monosulfide and disulfide molecular products.[28,29] Thus, we anticipate that metal sulfides will also be produced here. The present work reports the reaction of laser-ablated Fe, Ru, and Os atoms with small sulfur molecules $S_{1,2,3,4}$ produced through microwave discharge of elemental sulfur and sulfur-34 vapor[30] and density functional calculations of the anticipated metal sulfide product molecules.

## Experimental and Computational Methods

The technique for investigating reactions of laser-ablated metal atoms has been described in detail previously.[31] The Nd:YAG laser fundamental (1064 nm, 10 Hz repetition rate with 10 ns pulse width) was focused onto a rotating high-purity iron, ruthenium (Johnson Matthey), or osmium (E-Vac Products) metal target. The laser energy was varied from 5 to 10 mJ/pulse. Metal atoms were codeposited with a sulfur-doped argon stream onto a 7 K CsI cryogenic window at 2−4 mmol/h for 1 h. Infrared spectra were recorded at 0.5 $cm^{-1}$ resolution on a Nicolet 550 spectrometer with 0.1 $cm^{-1}$ accuracy using a

* To whom correspondence should be addressed. E-mail: lsa@virginia.edu.

10.1021/jp900994c CCC: $40.75 
Published on Web 03/30/2009

mercury cadmium telluride detector. Matrix samples were annealed at different temperatures, and selected samples were subjected to irradiation using a medium-pressure mercury lamp (>220 nm) with the globe removed.

A microwave discharge in argon seeded with sulfur vapor was used as a source of sulfur atoms and small molecules as reagents. The coaxial quartz discharge tubes used here evolved from the one described in earlier experiments.[30] Natural isotopic sulfur (Electronic Space Products, Inc., recrystallized) and enriched sulfur (98% $^{34}S$, Cambridge Isotope Laboratories) were used as received: different mixtures of the two isotopic samples were also employed. The vapor pressure of sulfur feeding the discharge was controlled by resistance heating. The microwave discharge maintained in the argon−sulfur mixture (Opthos Instruments 120 W microwave discharge, 30−50% of the maximum power level) with an Evenson−Broida cavity extended from 5 cm downstream of the sulfur reservoir to the end of the discharge tube.

Following previous work,[28,29,31,32] DFT calculations were performed on anticipated metal sulfide products first using the Gaussian 98 program,[33] the B3LYP or BPW91 density functional,[34,35] the 6-311+G(d) basis set for sulfur and iron, and the LanL2DZ effective core potential and basis for Ru and Os.[36,37] Additional calculations were performed using the Gaussian 03 program system,[38] the B3LYP density functional,[34] the large Gaussian basis 6-311+G(3df) for S and Fe, and the SDD pseudopotential and basis for Ru and Os atoms.[36,39]

## Results and Discussion

**Infrared Spectra.** Elemental sulfur vapor in a flowing argon discharge gives $S_2$ as judged from its blue emission[40] and $S_3$ and $S_4$ based on their known infrared absorption spectra.[30] Laser-ablated group 8 metal atoms were codeposited with such an argon stream, and new metal-dependent sulfur reaction product spectra will be presented and assigned. Relatively low laser energy was employed, and the concentration of metal atoms is sufficiently low as to minimize the contribution of dimetal species to the observed spectra: resolved natural ruthenium isotopic splittings support this point.

**Fe + $S_x$.** Five experiments were done with iron and sulfur vapor changing the sulfur content by a factor of 4 as judged by the strong $S_3$ absorption intensities and the ablation laser energy by a factor of 10 using a neutral-density filter. There were a large number of variables to control in these experiments. Representative spectra are illustrated in Figure 1, where the $S_3$ absorptions in the 600 $cm^{-1}$ region (not shown) are as intense as the $S_4$ absorptions, and weak $S_3$ bands are detected at 584.9, 581.7 $cm^{-1}$. The major absorptions appeared at 567.4, 540.2, 523.2, 467.2, and 461.8 $cm^{-1}$ as listed in Table 1. Annealing slightly increased the 540.2 and 467.2 $cm^{-1}$ and decreased the 523.2 and 461.8 $cm^{-1}$ bands and ultraviolet irradiation had little effect. Higher annealing decreased the 567.4 $cm^{-1}$ peak in favor of its 565.0 $cm^{-1}$ satellite. These new product absorptions exhibited 8 −13 $cm^{-1}$ shifts on sulfur-34 substitution and 32/34 isotopic frequency ratios appropriate for Fe−S vibrational modes. Figure 2 compares product spectra with mixed sulfur-32,34 and with sulfur-34 substitution. The mixed sulfur isotopic multiplets reveal product stoichiometric information. Notice that the 567.4 $cm^{-1}$ band reveals a sextet, the 540.2 $cm^{-1}$ band a triplet, and the 523.2 $cm^{-1}$ band a doublet. On higher temperature annealing, the sextet sharpens and gives way to a broad triplet, which corresponds to the 565.0 $cm^{-1}$ satellite in the original spectrum.

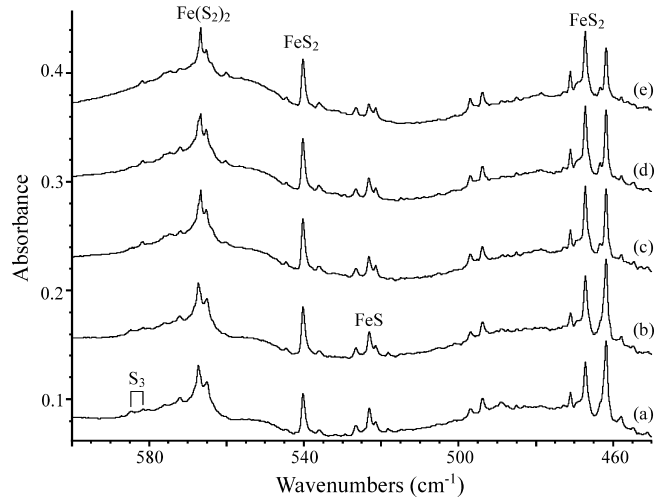


**Figure 1.** Infrared spectra in the 600−450 $cm^{-1}$ region for products formed in the laser-ablated Fe reaction with discharged sulfur vapor during condensation in excess argon at 7 K: (a) sample deposited for 60 min, (b) after annealing to 25 K, (c) after annealing to 35 K, (d) after >220 nm irradiation, and (e) after annealing to 40 K.

A very weak band at 542.1 $cm^{-1}$ becomes 5-fold stronger relative to the 540.2 $cm^{-1}$ band when the laser energy is reduced using a 10% neutral-density filter, as shown in Figure 3. This band is reduced substantially on full arc irradiation while the 540.2 $cm^{-1}$ band increases by 10%. The sulfur-34 counterpart at 534.4 $cm^{-1}$ defines a very low 1.0144 isotopic frequency ratio and decreases 50% on full arc irradiation while the 531.3 $cm^{-1}$ band increases 10%. Mixed isotopic spectra from an experiment using lower laser energy gave a 1/2/1 triplet absorption with 538.4 $cm^{-1}$ intermediate component for this photosensitive species.

**Ru + $S_x$.** Ruthenium atom reactions with the sulfur vapor mix gave spectra shown in Figure 4. The strongest features are a single band at 556.1 and the resolved ruthenium isotopic multiplet[27,41] terminated by the Ru-102 and 104 peaks at 535.5 and 533.9 $cm^{-1}$. Ultraviolet irradiation had no effect, but annealing slightly decreased the multiplet and increased the single band. A weaker ruthenium isotopic multiplet in the 540 $cm^{-1}$ region and a 518.7 $cm^{-1}$ band are also observed. These absorptions shifted with sulfur-34 substitution, and exhibited different sulfur isotopic frequency ratios as given in Table 2. Isotopic spectra illustrated in Figure 5 reveal triplet mixed sulfur isotopic spectra for the major bands.

**Os + $S_x$.** Osmium atom reaction product absorption spectra are shown in Figure 6 for natural sulfur-32, sulfur-34, and a mixture of the two. The band patterns are different for the two pure isotopic spectra owing to different isotopic shifts for the major product species (Table 2). The most straightforward is the lower region containing 503.7 and 491.6 $cm^{-1}$ bands for the pure isotopes and a slightly broadened lower band for the mixture. The upper region contains several overlapping mixed isotopic triplets, which will be discussed below. Figure 7 shows the behavior on annealing and UV irradiation in the sulfur-34 experiment where there is less band overlap: the stronger bands increase on annealing to 30 K, but UV irradiation decreases the upper bands in favor of the $OsS_4$ band.

**Calculations.** Density functional calculations were done for anticipated product molecules in different electronic states using different basis sets and pseudopotentials for the metals. The results of these calculations are summarized in Table 2 and discussed with each molecule below.

**TABLE 1: Infrared Absorptions ($cm^{-1}$) from Codeposition of Laser-Ablated Fe, Ru, and Os Atoms with Discharged Sulfur Vapor in Excess Argon**

| $^{32}S$ | $^{34}S$ | $^{32}S + {}^{34}S$ | $R$(32/34) | identity |
|---|---|---|---|---|
| | | Iron | | |
| 567.4 | 554.6 | 567.4, 564.4, 562.1, 561.2, 558.3, 554.6 | 1.0231 | $Fe(S_2)_2$ |
| 565.0 | 552.2 | 565.2, 559.0, 552.3 | 1.0232 | $Fe(S_2)_2$ isomer |
| 542.1 | 534.4 | 542.1, 538.4, 534.4 | 1.0144 | $FeS_2^-$ |
| 540.2 | 531.3 | 540.2, 536.1, 531.3 | 1.0168 | $FeS_2$, $\nu_3$ |
| 526.6 | 515.6 | | 1.0213 | |
| 523.2 | 513.4 | | 1.0191 | FeS |
| 518.3 | 508.6 | 518.3, 508.6 | 1.0191 | FeS site |
| 493.7 | | 483.8 | 1.0205 | $Fe_xS_y$ |
| 471.1 | 462.3 | | 1.0190 | |
| 467.2 | 457.2 | 467.2, 461.9, 457.5 | 1.0216 | $FeS_2$, $\nu_1$ |
| 461.8 | 453.1 | 457.5, 453.0 | 1.0190 | |
| | | Ruthenium | | |
| 572.0 | 556.3 | | 1.0282 | $Ru_x(S_2)$ |
| 569.7 | 553.5 | | 1.0293 | $Ru_x(S_2)$ site |
| 556.1 | 540.7 | 556.1, 548.4, 540.8 | 1.0285 | $Ru(S_2)$ |
| 546.1 | 535.6 | | 1.0196 | $^{99}RuS_3$ |
| 545.2 | 534.6 | | 1.0198 | $^{100}RuS_3$ |
| 544.2 | 533.6 | | 1.0199 | $^{101}RuS_3$ |
| 543.4 | 532.8 | | 1.0199 | $^{102}RuS_3$ |
| 541.5 | 531.0 | | 1.0198 | $^{104}RuS_3$ |
| 542.6 | 531.8 | | 1.0203 | $(S_2)RuS_2$, site |
| 540.8 | 530.1 | | 1.0202 | $(S_2)RuS_2$ $b_2$ |
| 537.9 | 527.1 | 537.9, −, 527.1 | 1.0205 | $^{99}RuS_2$, $\nu_3$ |
| 537.1 | 526.2 | −, −, 526.2 | 1.0207 | $^{100}RuS_2$, $\nu_3$ |
| 536.3 | 525.4 | −, 532.7, 525.4 | 1.0207 | $^{101}RuS_2$, $\nu_3$ |
| 535.5 | 524.6 | −, 531.9, 524.6 | 1.0208 | $^{102}RuS_2$, $\nu_3$ |
| 533.9 | 523.0 | −, 530.3, 523.0 | 1.0208 | $^{104}RuS_2$, $\nu_3$ |
| 518.7 | 506.3 | 518.5, 511.5, 506.8 | 1.0245 | $(S_2)RuS_2$ $a_1$ |
| | 481.5 | | | $[^{100}RuS_4]$ |
| 490 | 479.9 | | 1.021 | $[^{102}RuS_4]$ |
| | 478.5 | | | $[^{104}RuS_4]$ |
| | 475.5 | | | $[^{100}RuS_2^-]$ |
| | 473.9 | | | $[^{102}RuS_2^-]$ |
| | 472.5 | | | $[^{104}RuS_2^-]$ |
| | | Osmium | | |
| 546.9 | 531.2 | 546.9, 539.1, 531.2 | 1.0296 | $Os(S_2)$ |
| 545.1 | 532.6 | 545.1, 543.1, 532.6 | 1.0235 | $(S_2)OsS_2$ |
| 537.5 | 524.9 | | 1.0240 | $OsS_2$ |
| 536.8 | 522.6 | 536.9, 526.5, 522.6 | 1.0271 | $(S_2)OsS_2$ |
| 520.2 | 505.4 | 520.2, 513.7, 505.4 | 1.0293 | $(S_2)OsS_2$ |
| 503.7 | 491.6 | 503.7, 498.5, 495.9, 493.0, 491.6 | 1.0246 | $OsS_4$ |
| 492.4 | 479.9 | | 1.0260 | [OsS] |

**FeS.** The 523.2 $cm^{-1}$ band in iron−sulfur experiments decreases on annealing and shifts to 513.4 $cm^{-1}$ with sulfur-34, and this 32/34 isotopic frequency ratio, 1.0191, is in excellent agreement with the harmonic FeS diatomic isotopic frequency ratio (1.0192). The mixed sulfur isotopic spectrum (Figure 2) reveals a pure isotopic doublet, which shows conclusively that this absorption involves a single sulfur atom. The microwave spectrum finds a $^5\Delta$ ground state for FeS and predicts a 506 $cm^{-1}$ fundamental from centrifugal distortion constants,[21] while the high-resolution photoelectron spectrum also determined a $^5\Delta$ ground state with a 520 ± 30 $cm^{-1}$ vibrational spacing.[16] Theoretical calculations predict values 544, 532, 521, and 513 $cm^{-1}$ depending on the methods employed,[22−25] and our calculation gives 514 $cm^{-1}$. The early matrix isolation reaction of thermal Fe with OCS reveled 542 and 522 $cm^{-1}$ product absorptions in solid argon without isotopic substitution, and these workers assigned the 522 $cm^{-1}$ band to $SO_2$ impurity and the 542 $cm^{-1}$ band to FeS.[20] The $FeS_2$ molecule is identified here at 540.2 $cm^{-1}$ from mixed isotopic absorptions (see below),

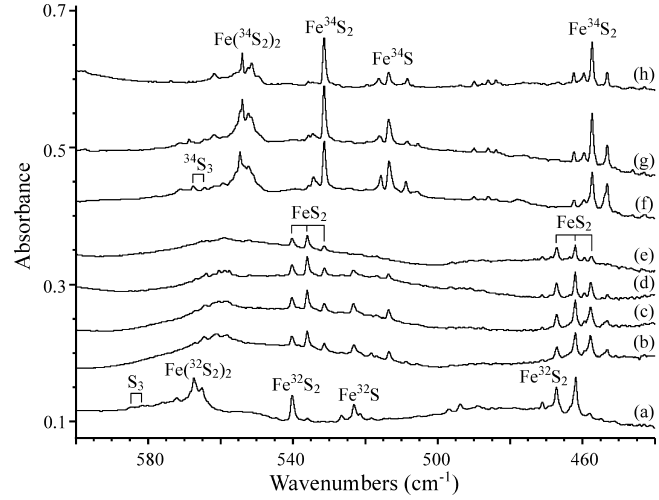


**Figure 2.** Infrared spectra in the 600−440 $cm^{-1}$ region for products formed in the laser-ablated Fe reaction with discharged sulfur-34 enriched vapor during condensation in excess argon at 7 K: (a) normal $^{32}S$ isotopic sample deposited for 60 min, (b) 50/50 mixed $^{32,34}S$ isotopic sample, (c) after annealing to 30 K, (d) after annealing to 40 K, (e) after annealing to 48 K, (f) $^{34}S$ after sample deposition, (g) after annealing to 5 K, and (h) (c) after annealing to 43 K.

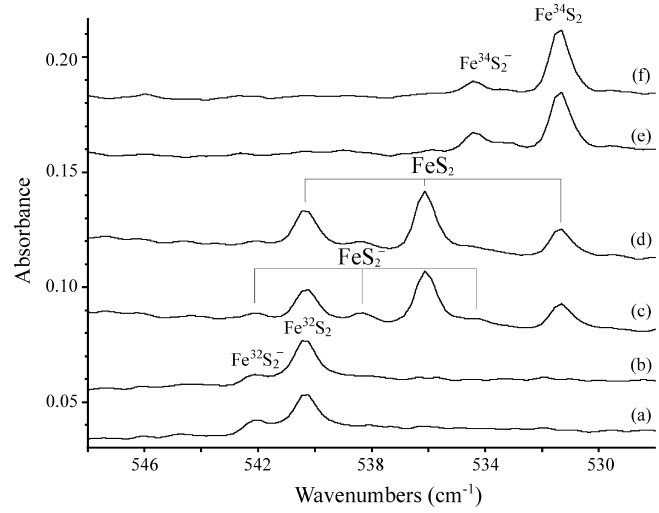


**Figure 3.** Infrared spectra in the 550−530 $cm^{-1}$ region for products formed in the low-energy laser-ablated Fe reaction with discharged sulfur vapor during condensation in excess argon at 7 K: (a) normal $^{32}S$ isotopic sample deposited for 60 min, (b) after >220 nm irradiation, (c) 50/50 mixed $^{32,34}S$ isotopic sample, (d) after >220 nm irradiation, (e) $^{34}S$ after sample deposition, and (f) after >220 nm irradiation.

and the previous 542 $cm^{-1}$ band could be due to $FeS_2$. Without benefit of isotopic mixtures, these workers also reversed the identifications of VS and $VS_2$ reaction products.[28] In summary, the present 523.2 $cm^{-1}$ band is assigned to the FeS vibrational fundamental in solid argon on the basis of the foregoing evidence, particularly sulfur-34 substitution. It is difficult to predict the gas-phase fundamental from this single observation, but we certainly expect it to be within 10 $cm^{-1}$ of our argon matrix value. The FeS molecule is probably produced here from the combination of Fe and S atoms during formation of the argon matrix, which attests to the deposition of S atoms from the discharge source.

**$FeS_2$.** The 540.2 $cm^{-1}$ absorption increases slightly on annealing and shifts to 531.3 $cm^{-1}$ on sulfur-34 substitution, and the isotopic frequency ratio so defined (1.0168) reveals less sulfur participation in this vibrational mode than for the above FeS diatomic molecule. This can arise from more involvement

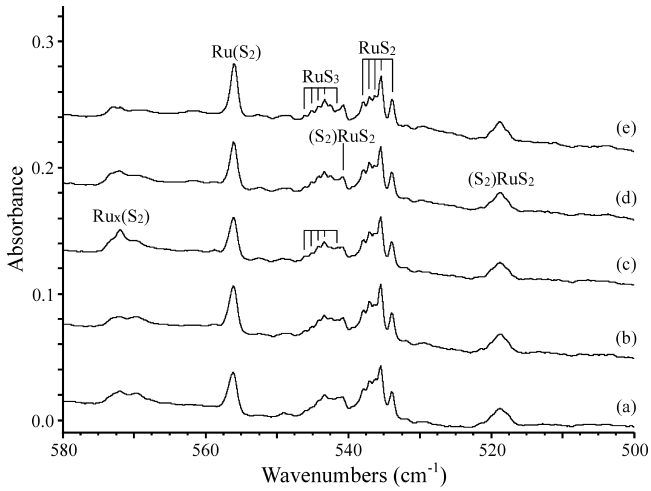


**Figure 4.** Infrared spectra in the 580−500 $cm^{-1}$ region for products formed in the laser-ablated Ru reaction with discharged sulfur vapor during condensation in excess argon at 7 K: (a) sample deposited for 60 min, (b) after annealing to 30 K, (c) after >220 nm irradiation, (d) after annealing to 35 K, and (e) after annealing to 40 K.

of Fe in the antisymmetric motion between two S atoms. The mixed isotopic spectrum reveals a triplet pattern at 540.2, 536.1, 531.3 $cm^{-1}$, and the stronger single intermediate component characterizes the motion of two equivalent sulfur atoms. It is significant that the intermediate component is higher (0.3 $cm^{-1}$) than the average of pure isotopic bands (535.8 $cm^{-1}$) as this points to interaction with the lower frequency symmetric stretching mode of the mixed isotopic molecule, which now are of the same symmetry. Our best calculation (6-311+(3df) basis) for $FeS_2$ finds the $^5B_2$ ground state, in agreement with previous workers,[18] and the strong $b_2$ mode at 546.8 $cm^{-1}$ with a weaker $a_1$ mode at 476.1 $cm^{-1}$ (Table 2). The computed 32/34 isotopic frequency ratios for the $b_2$ and $a_1$ modes of this molecule of angle 113.5° are 1.0167 and 1.0219, respectively. The agreement of the 540.2 $cm^{-1}$ observed band and isotopic characteristics with the computed $b_2$ mode values for the $^5B_2$ ground state is sufficient to confirm the identification of the open iron disulfide molecule; however, there is more information. The 467.2 $cm^{-1}$ band tracks with the 540.2 $cm^{-1}$ band on annealing, but it is slightly stronger, and our calculation predicted a weaker symmetric stretching mode for $FeS_2$. The 467.2 $cm^{-1}$ band shifts to 457.2 $cm^{-1}$ (ratio 1.0216) and forms a mixed isotopic triplet although there is overlap with components for the 461.8 $cm^{-1}$ band. Significantly, the 461.9 $cm^{-1}$ intermediate component is 0.3 $cm^{-1}$ lower than the average of the pure isotopic bands precisely matching the 0.3 $cm^{-1}$ higher intermediate component in the antisymmetric stretching mode triplet absorption. This is due to coupling of the two stretching modes of $^{32}SFe^{34}S$, which now have the same symmetry. The 467.2 $cm^{-1}$ band and isotopic counterparts are also in excellent agreement with computed $a_1$ mode values for the $FeS_2$ molecule and add further support for its identification. Our B3LYP calculation describes this quintet ground state amazingly well: there is little spin contamination [$\langle S(S+1)\rangle$ is 6.18 before and 6.00 after annihilation].

**$FeS_2^-$.** The weak 542.1 $cm^{-1}$ band increases in intensity relative to the strong $FeS_2$ absorption at 540.2 $cm^{-1}$ with reduced laser energy, and full arc irradiation reduces the former and increases the latter absorptions (Figure 3), which are characteristic of a molecular anion.[31a,42] The photosensitive 542.1 $cm^{-1}$ band shifts to 534.4 $cm^{-1}$ with sulfur-34 and forms a 1/2/1 triplet with median 538.4 $cm^{-1}$ band using mixed isotopes. This triplet characterizes the vibration of two equivalent sulfur atoms, and the low 32/34 isotopic frequency ratio 1.0144 indicates the increased involvement of the Fe partner as would be found with a larger obtuse angle. Anion photodetachment indicates that $FeS_2^-$ is a very stable anion ($FeS_2$ electron affinity 74.3 kcal/mol), and B3LYP calculations have predicted a nearly linear $^6A_1$ iron disulfide anion structure.[16,18] Using a larger basis set, our DFT calculation predicts almost the same structure, an electron affinity of 74.5 kcal/mol, and a very strong antisymmetric mode at 529.6 $cm^{-1}$ with isotopic 32/34 ratio 1.0142. In addition, the calculated mixed 32,34 isotopic component is 0.1 $cm^{-1}$ above the median of pure isotopic values, just as is the observed value. Hence, the weak 542.1 $cm^{-1}$ band can be assigned to the iron disulfide molecular anion made here by electron capture during codeposition of laser-ablated iron atoms and electrons with sulfur molecules. It is perhaps fortuitous that DFT/B3LYP calculations work so well for the nearly linear $^6A_1$ iron disulfide anion in view of the fact that the isoelectronic $FeO_2^-$ anion is a linear doublet ground state and a multireference computational problem.[42c] Our B3LYP calculation predicts a sextet state with no spin contamination [$\langle S(S+1)\rangle$ is 8.78 before and 8.75 after annihilation].We invite higher level calculations to confirm this assignment and application of the single reference DFT method.

**$Fe(S_2)$.** Our best calculation finds a $^5A_1$ ground state for the side-bound $Fe(S_2)$ complex (Table 2), which is 3 kcal/mol lower energy than the above $^5B_2$ ground state of the open disulfide molecule, in disagreement with earlier workers who used a smaller basis set.[18] However, this energy is within the accuracy of our calculation, and these two states have almost the same energy. Most importantly, this side-bound $Fe(S_2)$ complex has its strongest computed mode at 477.7 $cm^{-1}$ and this mode has more S−S stretching character and a higher 32/34 ratio (1.0234), which is not compatible with the observed 476.2 $cm^{-1}$ band. In addition, the mixed isotopic band in the case of the $Fe(S_2)$ complex is expected to be higher than the median isotopic band because the interacting partner is computed to be lower (Table 2), and such is not the case. Hence, we have no evidence for the $Fe(S_2)$ complex in our experiment. The calculated structure for the $Fe(S_2)$ complex reveals an S−S distance close to that in iron pyrite (2.171 Å), but our Fe−S distance is shorter than the solid value (2.259 Å).[2] The most stable form of iron trisulfide is $SFe(S_2)$ (Table 2), but we do not have evidence for this molecule either.

**$Fe(S_2)_2$.** The highest new band at 567.4 $cm^{-1}$ shifts to 554.6 $cm^{-1}$ with sulfur-34 and defines a 1.0231 ratio, which suggests a mixed S−S and Fe−S stretching mode. The mixed sulfur 32,34 sample gave a partially resolved sextet, which sharpened on annealing and then gave way to a broad triplet at 565.2, 559.0, 552.3 $cm^{-1}$. This triplet characterizes the 565.0 $cm^{-1}$ satellite absorption as being due to a species with two almost equivalent $S_2$ subunits where each gives a triplet mixed isotopic band and the two almost overlap. The sextet is expected for two equivalent $S_2$ subunits each with equivalent S atoms, which has been observed with textbook 1/4/4/2/4/1 relative intensities for the group 10 metal atom and $S_2$ reactions.[43] The most stable iron tetrasulfide stoichiometry molecules we converged after many attempts are the $Fe(S_2)_2$ structures detailed in Table 2. These have intense high-frequency mixed S−S and Fe−S stretching modes computed at 579 or 547 $cm^{-1}$. The former $^5B_1$ species has a computed mixed isotopic sextet, which fits the 567.4 $cm^{-1}$ band very well. This quintet state is not spin contaminated [$\langle S(S+1)\rangle$ is 6.11 before and 6.00 after annihilation]. The latter $^3B_1$ state exhibits a calculated mixed

**TABLE 2: Calculated Structural Parameters and Vibrational Frequencies ($cm^{-1}$) for Group 8 Sulfide Molecules and Complexes[a]**

| species | state | lengths (Å) angles (deg) | rel energy (kcal/mol) | freq ($cm^{-1}$) (symmetry, intensities, km/mol) |
|---|---|---|---|---|
| $S_2$ | $^3\Sigma_g^-$ | SS: 1.902 | 0 | 715.9 (0) |
| $S_3$ | $^1A_1$ | SS: 1.922<br>SSS: 118.5 | 0 | 686.5($b_2$,134), 594.5($a_1$,2), 262.3($a_1$,1) |
| iron | | | | |
| FeS | $^5\Delta$ | FeS: 2.028 | 0 | $Fe^{32}S$: 514.5(30); $Fe^{34}S$: 504.8(29) |
| FeS | $^5\Sigma^+$ | FeS: 2.004 | +5 | $Fe^{32}S$: 528.0(39); $Fe^{34}S$: 518.1(38) |
| $FeS^-$ | $^6\Delta$ | FeS: 2.137 | −34 | $Fe^{32}S$: 451.6(105); $Fe^{34}S$: 443.1(99) |
| $Fe(S_2)$ | $^5A_1$ | FeS: 2.166<br>SS: 2.180 | 0 | 477.3 ($a_1$,29), 331.8 ($b_2$,3), 297.9($a_1$,2) |
| $FeS_2$ | $^5B_2$ | FeS: 2.013<br>SFeS: 113.5 | +3 | $Fe^{32}S_2$: 546.8($b_2$,32), 476.1($a_1$,13), 126.7($a_1$,2)<br>$Fe^{32}S^{34}S$: 542.6(a,31), 470.7(a, 12), 125.3(a,2)<br>$Fe^{34}S_2$: 537.8($b_2$,31), 465.9($a_1$,12), 123.9($a_1$,2) |
| $FeS_2$ | $^3B_1$ | FeS: 2.056<br>SFeS: 146.3 | +20 | $Fe^{32}S_2$: 471.5($b_2$,41), 357.9($a_1$,6), 49.8($a_1$,3) |
| $Fe(S_2)$ | $^5B_1$ | FeS: 2.330<br>SS: 2.082 | 22 | 509 ($a_1$,6), 241 ($b_2$,0), 237($a_1$,8) |
| $FeS_2$<br>[SDD for Fe] | $^5B_2$ | FeS: 2.013<br>SFeS:112.9 | | $Fe^{32}S_2$: 537.5($b_2$,25), 465.1($a_1$,13), 124.3($a_1$,2) |
| *SFe*($S_2$) | $^3B_1$ | FeS: 2.091, 2.339<br>SS: 2.003 | 0 | $Fe^{32}S_2$: 592 ($a_1$,45), 419($a_1$,1), 242($a_1$,11) |
| *FeS*$_3$ ($D_{3h}$) | $^1A_1'$ | FeS: 1.937 | *45* | 631 (e,47 × 2), 489 ($a_1$,0), 187 (e,7 × 2), 112 ($a_2''$,0) |
| $FeS_2^-$ | $^6A_1$ | FeS: 2.117<br>SFeS: 169.7 | −72 | $Fe^{32}S_2$: 529.6($b_2$,169), 389.8($a_1$,1), 29.7($a_1$,33)<br>$Fe^{32}S^{34}S$: 526.0(a,166), 383.9(a,1), 29.5(a,32)<br>$Fe^{34}S_2$: 522.2($b_2$,162), 378.3($a_1$,1), 29.3($a_1$,31) |
| $Fe(S_2)_2$ ($D_2$)<br>[ SDD for Fe] | $^5B_1$ | FeS: 2.218<br>SS: 2.0230 | 578.9 ($b_3$,61), 569(a,0), 348($b_2$,0), 330 ($b_3$,52) | [576.4, 575.5, 571.1, 568.5, 563.1 ($b_3$) for $^{34}S_{1,2,2,3,4}$] |
| $Fe(S_2)_2$ ($C_{2v}$)<br>[ SDD for Fe] | $^3B_1$ | FeS: 2.179, 2.285<br>SS: 2.049, 1.9940 | 600.0 ($a_1$,24), 546.7($b_2$, 133) | [546.1, 540.0, 546.3, 539.9, 533.2, 539.7, 533.1, 532.9 ($b_2$) for $^{34}S_{1,2,2,3,4}$ in order] |
| $FeS_4$ ($T_d$) | $^1A_1$ | FeS: 1.988 | 105 | 517($t_2$,62 × 3), 462($a_1$,0), 242($t_2$,5 × 3), 193(e,0 × 2) |
| Ruthenium | | | | |
| *RuS* | $^5\Delta$ | RuS: 2.134 | | $^{100}$RuS: 479.5, $^{102}$RuS: 478.3(26), $^{104}$RuS; 477.2 |
| *RuS* | $^5\Sigma^+$ | RuS: 2.145 | 14 | $^{102}Ru^{32}S$: 474.1(17), $^{102}Ru^{34}S$: 463.4(16) |
| $RuS_2$ | $^3B_1$ | RuS: 2.063<br>SRuS: 119.9 | 0 | $^{102}Ru^{32}S_2$: 550.5($b_2$,78),526.3($a_1$,9), 127.9 ($a_1$,1)<br>$^{102}Ru^{32}S^{34}S$: 546.3(a,74), 518.3(a,12), 126.5(a,1)<br>$^{102}Ru^{34}S_2$: 539.4($b_2$,75),513.0($a_1$,9), 125.0 ($a_1$,1) |
| $RuS_2$ | $^5B_2$ | RuS: 2.108 SRuS: 111.4 | 2 | $^{102}Ru^{32}S_2$: 500.4($a_1$,8),495.1($b_2$,31), 155.4 ($a_1$, 1) |
| *RuS*$_2$ | $^3B_1$ | RuS: 2.089<br>SRuS: 117.5 | *0* | $^{100}Ru^{32}S_2$: 531.8($b_2$,78),504.8($a_1$,11), 125.4 ($a_1$, 1)<br>$^{102}Ru^{32}S_2$: 530.2($b_2$,78), 504.0($a_1$,11), 125.1($a_1$,1)<br>$^{104}Ru^{32}S_2$: 528.6($b_2$,78),503.3($a_1$,11), 124.8 ($a_1$,1) |
| $RuS_2^-$ | $^4B_2$ | RuS: 2.134<br>SRuS: 122.1 | −29 | $^{100}Ru^{32}S_2$: 483.5($b_2$,139),463.2($a_1$,18), 106.4 ($a_1$,2)<br>$^{102}Ru^{32}S_2$: 481.9($b_2$,139),462.5($a_1$,18), 106.1 ($a_1$,2)<br>$^{104}Ru^{32}S_2$: 480.4($b_2$,138),461.8($a_1$,18), 105.9 ($a_1$,2) |
| $RuS_2^-$ | $^6A_1$ | RuS: 2.215<br>SRuS: 135.7 | −16 | $^{102}Ru^{32}S_2$: 423.8($b_2$,98),409.1($a_1$,8), 104.1 ($a_1$,3) |
| $Ru(S_2)$ | $^3A_2$ | RuS: 2.271<br>SS: 2.037 | 14 | $^{102}Ru^{32}S_2$: 549.7 ($a_1$,15), 362.1($a_1$,2), 238.4($b_2$,4)<br>$^{102}Ru^{32}S^{34}S$: 541.8(a,14), 358.7(a,2), 235.2(a,4)<br>$^{102}Ru^{34}S_2$: 533.7 ($a_1$,14), 355.3($a_1$,2), 232.1($b_2$,4) |
| $Ru(S_2)$ | $^5A_1$ | RuS: 2.252<br>SS: 2.206 | 27 | $^{102}Ru^{32}S_2$: 471.3 ($a_1$,14), 208.0($a_1$,0), 186.6($b_2$,1) |
| *Ru* ($S_2$) | $^3A_2$ | RuS: 2.318<br>SS: 2.074 | 8 | $^{102}Ru^{32}S_2$: 522.7 ($a_1$,17), 341.7($a_1$,3), 228.6($b_2$,7) |
| *RuS*$_3$ ($D_{3h}$) | $^1A_1'$ | RuS: 2.084 | 0 | 549 (e,50 × 2), 464 ($a_1$,0), 160 (e,4 × 2), 73 ($a_2''$,0) |
| $SRu(S_2)$ | $^3B_1$ | RuS: 2.127, 2.450<br>SS: 2.003 | 13 | $^{102}Ru^{32}S_2$: 586 ($a_1$,32), 488($a_1$,53), 243($a_1$,7) |
| $(S_2)RuS_2$ ($C_{2v}$)<br>nonplanar | $^1A_1$ | RuS: 2.083<br>SRuS: 116.0<br>RuS: 2.311<br>SS: 2.0820 | 0 | $^{102}Ru^{32}S_2$: 542.8($b_2$,66),530.3($a_1$,77), 514.6 ($a_1$,8)<br>$^{102}Ru^{34}S_2$: 532.1 ($b_2$,65), 516.6($a_1$75), 500.9($a_1$,7) |
| *RuS*$_4$ ($T_d$) | $^1A_1$ | RuS: 2.126 | 19 | 483($t_2$,50 × 3), 464($a_1$,0), 201($t_2$,3 × 3), 180(e,0 × 2) |
| $(S_2)RuS_2$ ($C_{2v}$)<br>nonplanar | $^1A_1$ | RuS: 2.067<br>RuS: 116.1<br>RuS: 2.274<br>SS: 2.0510 | | $^{102}Ru^{32}S_2$: 559.0($b_2$,69),555.2($a_1$,64), 532.7 ($a_1$, 24)<br>$^{102}Ru^{34}S_2$: 548.0 ($b_2$,66), 539.9($a_1$66), 519.4($a_1$,17) |
| $RuS_4$ ($T_d$) | $^1A_1$ | RuS: 2.105 | 19 | 511($t_2$,57 × 3), 488($a_1$,0), 209($t_2$,2 × 3), 185(e,0 × 2) |
| osmium | | | | |
| *OsS* | $^5\Sigma^+$ | OsS: 2.12 | 0 | $Os^{32}S$: 509.3(9); $Os^{34}S$: 496.3(8) |
| *OsS* | $^5\Delta$ | OsS: 2.13 | 9 | $Os^{32}S$: 494.2(16); $Os^{34}S$: 481.7(8) |

**TABLE 2: Continued**

| species | state | lengths (Å) angles (deg) | rel energy (kcal/mol) | freq ($cm^{-1}$) (symmetry, intensities, km/mol) |
|---|---|---|---|---|
| $OsS_2$ | $^3B_1$ | OsS: 2.078<br>SRuS: 122.2 | 0 | $Os^{32}S_2$: 547.4($a_1$,6), 538.8($b_2$,67), 138.1 ($a_1$,1)<br>$Os^{32}S^{34}S$: 544.0(a,22), 528.3(a,49), 136.4(a,0)<br>$Os^{34}S_2$: 532.5($a_1$,6),526.1($b_2$,64), 134.7 ($a_1$,1) |
| $OsS_2^-$ | $^4B_2$ | OsS: 2.142<br>SRuS: 121.3 | −56 | $Os^{32}S_2$: 486 ($a_1$,12), 476($b_2$,99), 124 ($a_1$, 2) |
| $Os(S_2)$ | $^3A_2$ | OsS: 2.274<br>SS: 2.047 | 44 | $Os^{32}S_2$: 546.0 ($a_1$,15), 360.8($a_1$,0), 226.9($b_2$,2) $Os^{32}S^{34}S$: 538.1(a,15), 356.8(a,0), 223.7(a,2) $s^{34}S_2$: 530.0 ($a_1$,15), 352.6($a_1$,0), 220.6($b_2$,2) |
| $Os(S_2)$ | $^1A_1$ | OsS: 2.210<br>SS: 2.007 | 48 | $Os^{32}S_2$: 590.7 ($a_1$,9), 389.6($a_1$,0), 223.9($b_2$,) |
| $OsS_4$ ($T_d$) | $^1A_1$ | OsS: 2.128 | 0 | 512.5($a_1$,0), 500.5($t_2$,58 × 3), 194.0($t_2$,2 × 3), 186.2(e,0 × 2) |
| $(S_2)OsS_2$ ($C_{2v}$) nonplanar | $^1A_1$ | OsS: 2.312, 2.097<br>SS: 2.108<br>SOsS: 129.8 | 3 | $(S_2)Os^{32}S_2$: 545.3($b_1$,61), 537.3($a_1$,38), 523.0 ($a_1$, 36), 337.3($a_1$,3), 281.7($b_1$,3), 162.8($a_1$,0)<br>$(^{32}S_2)Os^{32}S^{34}S$: 542.6(a,61), 526.4(a,38), 522.9(a,36)<br>$(^{32}S^{34}S)Os^{32}S_2$: 545.3($b_1$,61), 537.3($a_1$,38), 515.4 ($a_1$,36) |

[a] Calculations used B3LYP/6-311+G(3df) for Fe and B3LYP/6-311+G(3df)/SDD for Ru and Os except where the formulas are in italics and B3LYP/6-311+G(d)/LANL was used.

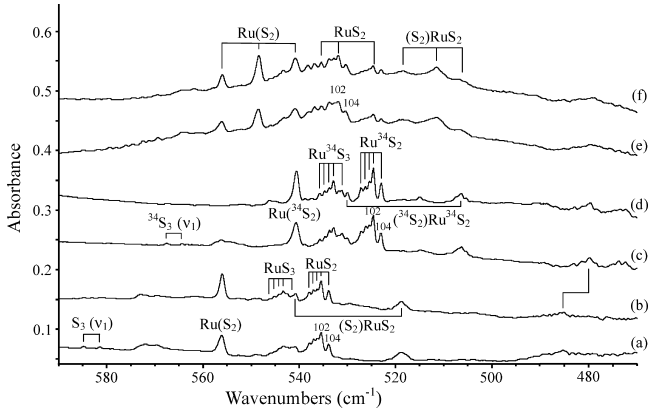


**Figure 5.** Infrared spectra in the 590−470 $cm^{-1}$ region for products formed in the laser-ablated Ru reaction with discharged sulfur vapor during condensation in excess argon at 7 K: (a) normal $^{32}S$ sample deposited for 60 min and (b) after annealing to 30 K, (c) $^{34}S$ sample after deposition and (d) after annealing to 30 K, (e) 50/50 mixed $^{32,34}S$ isotopic sample after deposition, and (f) after annealing to 30 K.

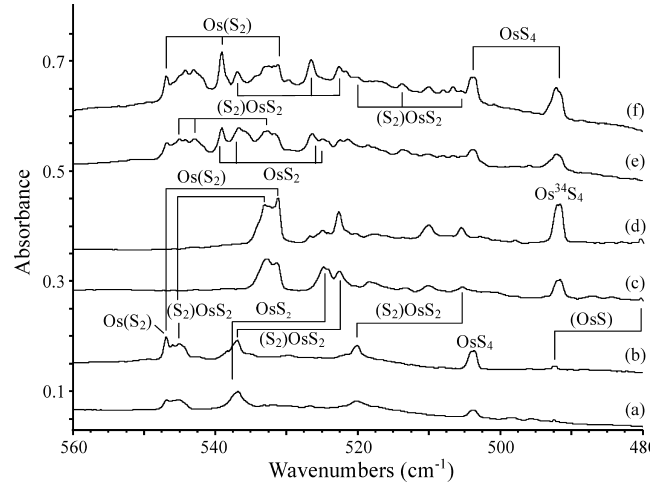


**Figure 6.** Infrared spectra in the 560−480 $cm^{-1}$ region for products formed in the laser-ablated Os reaction with discharged sulfur vapor during condensation in excess argon at 7 K: (a) normal $^{32}S$ sample deposited for 60 min and (b) after annealing to 40 K, (c) $^{34}S$ sample after deposition and (d) after annealing to 40 K, (e) 50/50 mixed $^{32,34}S$ isotopic sample after deposition, and (f) after annealing to 40 K.

isotopic triplet, which is appropriate for the 565.0 $cm^{-1}$ satellite absorption, but this calculation is an approximation as spin contamination is evident [$\langle S(S+1)\rangle$ is 3.07 before and 2.24 after annihilation].

**Other Absorptions.** Several other absorptions in Table 1 cannot be identified from the information available. The weak 526.6 $cm^{-1}$ absorption appears to be favored at lower laser energy, and the mixed isotopic spectrum reveals an intermediate component, so two sulfur atoms are likely. The 461.8 $cm^{-1}$ band is favored at higher laser energy, but it decreases on annealing. Overlapping of bands in the mixed isotopic experiments make the identification of intermediate components less than straightforward, but it appears that a mixed isotopic counterpart falls under the 457.2 $cm^{-1}$ $Fe^{34}S_2$ band. We considered cyclic $Fe_2S_2$ as a possibility because of the unique (diatomic FeS) sulfur 32/34 isotopic frequency ratio, but our DFT calculation finds a $^9A$ state with highest observable frequency at 426 $cm^{-1}$.

**$RuS_2$.** The resolved ruthenium natural isotopic quintet from 533.9 to 537.9 $cm^{-1}$ (Figure 4, Table 1) with natural abundance isotopic intensities is characteristic of the stretching mode of a single Ru atom.[27,41] The quintet shifts almost 11 $cm^{-1}$ upon sulfur-34 substitution, and the sulfur 32/34 isotopic ratios range from 1.0208 to 1.0205 as the Ru mass decreases from 104 to 99 and the lighter metal atom contributes more to the vibrational reduced mass. The mixed sulfur 32,34 reaction gave a triplet of quintets with some overlap (Figure 5, most intense Ru-102 positions marked). The ruthenium-102 mixed sulfur 32, 34 band at 531.9 $cm^{-1}$ is 1.8 $cm^{-1}$ higher than the median of pure sulfur isotopic bands, which demonstrates interaction with a relatively close lower frequency stretching mode now allowed in the lower symmetry mixed isotopic molecule.

Our B3LYP/6-311+G(3df)/SDD calculation for $RuS_2$ predicts a $^3B_1$ ground state with intense 550.5 $cm^{-1}$ antisymmetric stretching frequency and 1.0206 sulfur 32/34 ratio while the B3LYP/6-311+G(d)/LANL calculation finds a 530.2 $cm^{-1}$ frequency with 1.0208 sulfur 32/34 ratio and 3.2 $cm^{-1}$ Ru 100−104 separation (3.2 $cm^{-1}$ observed). Although the $^5B_2$ state was observed for $FeS_2$ and it is only 0−2 kcal/mol higher than the $^3B_1$ state for $RuS_2$, depending on the basis set, the strong computed frequency for the $^5B_2$ state, 495 $cm^{-1}$, is much lower than the observed value. Hence, we assign the ruthenium natural isotopic quintet from 533.9 to 537.9 $cm^{-1}$ to the $^3B_1$ ground state of $RuS_2$ in the argon matrix. The much weaker symmetric stretching mode, predicted in the low 500 $cm^{-1}$ region, is not observed. The B3LYP calculation describes this triplet ground state with no spin contamination [$\langle S(S+1)\rangle$ are 2.01 before and 2.00 after annihilation].

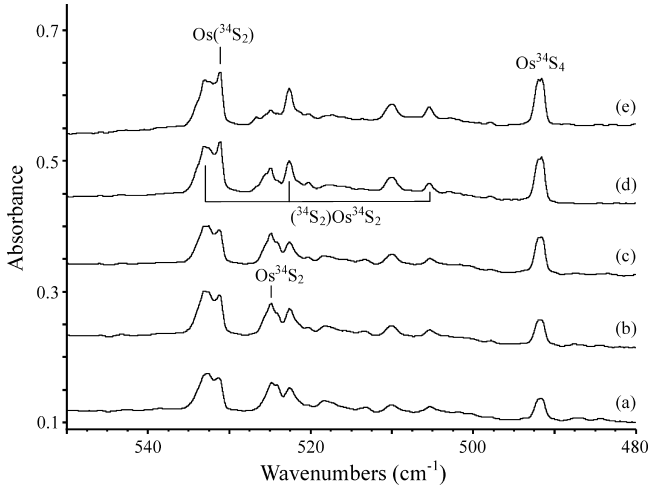


**Figure 7.** Infrared spectra in the 550−480 $cm^{-1}$ region for products formed in the laser-ablated Os reaction with discharged sulfur-34 vapor during condensation in excess argon at 7 K: (a) sample deposited for 60 min, (b) after annealing to 30 K, (c) after >220 nm irradiation, (d) after annealing to 35 K, and (e) after annealing to 40 K.

The isotopic frequencies for central and terminal isotopic substitution in the antisymmetric stretching mode for a $C_{2v}$ molecule can be used to estimate the valence angle, as detailed for the $S_3$ molecule.[30] Using the ruthenium isotopic data, a 112 ± 2° lower limit and using the sulfur isotopic data, a 117 ± 1° upper limit are predicted. These experimental values are in excellent agreement with the 117.5° and 119.9° values computed for the $^3B_1$ state of $RuS_2$, depending on the basis set.

**$Ru(S)_2$.** The strong single band at 556.1 $cm^{-1}$ shifts to 540.7 $cm^{-1}$ with sulfur-34 and defines a larger 32/34 ratio, 1.0285, which is characteristic of a S−S vibrational mode, hence no ruthenium isotopic structure. In the mixed 32, 34 isotopic experiment, a symmetrical triplet is observed with 548.4 $cm^{-1}$ intermediate component at the median position. This means that two equivalent sulfur atoms are involved and there is no nearby stretching mode to interact in the lower symmetry mixed isotopic molecule.

The B3LYP/6-311+G(3df)/SDD calculation for $Ru(S)_2$ predicts a $^3A_2$ ground state with medium intensity 549.7 $cm^{-1}$ symmetric stretching frequency and 1.0300 harmonic sulfur 32/34 isotopic frequency ratio. The slightly lower observed value is due to weak interaction with the symmetric Ru−S stretching mode predicted at 362 $cm^{-1}$. The antisymmetric Ru−S stretching mode is computed at 238 $cm^{-1}$, which is too low to interact with the higher symmetric modes in the mixed isotopic molecule of lower symmetry. In addition, the $^5A_1$ state is 14 kcal/mol higher energy, and the leading mode at 471 $cm^{-1}$ is too low for assignment to the observed band. The very good agreement between observed and computed vibrational characteristics for $Ru(S_2)$ in the $^3A_2$ ground state confirms its identification.

**$RuS_3$.** A weaker resolved ruthenium natural isotopic quintet from 541.5 to 546.1 $cm^{-1}$ is 8 $cm^{-1}$ higher than in the $RuS_2$ quintet. The ruthenium isotopic splittings are the same within experimental error, but the sulfur 32/34 frequency ratio is slightly lower for the weaker quintet suggesting a slightly larger obtuse valence angle for this product molecule with a similar antisymmetric Ru−S stretching mode in isotopic character. Our B3LYP/6-311+G(d)/LANL calculation for $RuS_3$ predicts a $^1A_1'$ ground state in $D_{3h}$ symmetry with intense antisymmetric stretching frequency 19 $cm^{-1}$ higher than $RuS_2$ and 1.0197 sulfur 32/34 ratio. Unfortunately, the mixed sulfur 32,34 spectrum of the disulfide covers this region. The weaker ruthenium isotopic quintet is assigned to $RuS_3$ on the basis of its observed and calculated relationship with that for $RuS_2$.

**$(S_2)RuS_2$.** Our B3LYP/6-311+G(d)/LANL calculation finds the lowest energy structure for ruthenium tetrasulfide to have the $^1A_1$ ground state in the nonplanar $C_{2v}$ structure with strong absorptions at 543 $cm^{-1}$ ($b_2$) and 530 $cm^{-1}$ ($a_1$). The tetrahedral structure is 19 kcal/mol higher with strong stretching mode at 483 $cm^{-1}$. The 540.8 $cm^{-1}$ peak appears to be the Ru-102 absorption for a multiplet that is mostly covered by the multiplet for $RuS_3$. This band exhibits the 32/34 isotopic ratio 1.0202, which is characteristic of an antisymmetric S−Ru−S stretching mode. The stronger and broader 518.7 $cm^{-1}$ band shows a 1.0245 isotopic 32/34 ratio and a broadened asymmetric triplet mixed sulfur isotopic band with intermediate component 1.2 $cm^{-1}$ below the pure isotopic median value, which indicates interaction with two additional equivalent sulfur atoms and a higher mode in the lower symmetry molecule. The 1.0245 isotopic frequency ratio characterizes a mixed Ru−S, S−S stretching mode. Our calculation predicts 32/34 isotopic ratios 1.0201 and 1.0265 for the above $b_2$ and $a_1$ modes, which considering the approximation involved, is very good agreement with the observed frequencies and isotopic data.

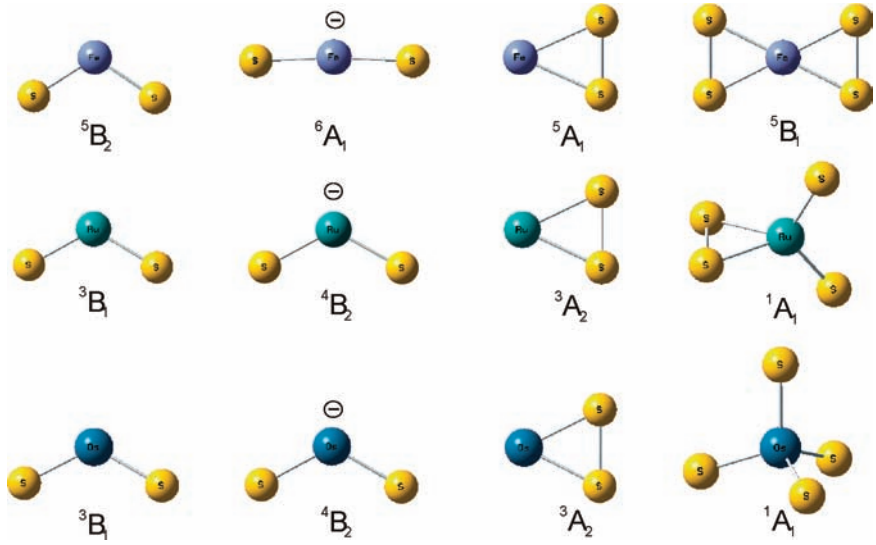


**Figure 8.** Structures calculated (B3LYP/6-311+G(3df)/SDD) for group 8 metal sulfur species.

**Weak Low-Frequency Absorptions: $RuS_4$. and $RuS_2^-$.** We observed the three strongest ruthenium isotopic components (Ru-100, -102, -104) at 481.5, 479.9, and 478.5 $cm^{-1}$ for a weak absorption in the most productive experiment, which used sulfur-34. This is where tetrahedral $RuS_4$ is expected to absorb, and our calculation predicts a 3.0 $cm^{-1}$ Ru 100-104 shift, which is in agreement with the observed band separation. The weak absorptions increased 50% on UV irradiation and decreased on higher temperature annealing and are tentatively assigned to the higher energy $RuS_4$ structural isomer. A weaker sulfur-32 counterpart was detected at 490 $cm^{-1}$. Recall that $RuO_4$ was observed in the corresponding oxygen investigation at 96.4% of the $OsO_4$ frequency, and 490 $cm^{-1}$ is 97.4% of the $OsS_4$ frequency to be assigned below.[27] Calculations with SDD tend to overestimate and with LANL tend to underestimate the observed $RuS_2$ frequency, and this molecule is a case in point (Table 2). Our calculation using SDD gave 511 $cm^{-1}$, in agreement with previous work,[44] and using LANL found 483 $cm^{-1}$: the computed values bracket the 490 $cm^{-1}$ observed frequency in the same way found for $RuS_2$.

Three additional weak absorptions with similar profile at 475.5, 473.9, 472.5 $cm^{-1}$ were almost destroyed by UV photolysis, and these are within a few $cm^{-1}$ of the position computed for the very strong $b_2$ mode of $^4B_2$ ground-state $RuS_2^-$, and the 3.1 $cm^{-1}$ predicted Ru 100−104 separation is in agreement with the observed band splitting. These bands are appropriate for the anion assignment, but without more observations, this must be considered tentative. The photosensitive $RuO_2^-$ anion was also observed in the earlier experiments.[27]

Our DFT calculation finds a $^5\Delta$ ground state for RuS with a 478.3 $cm^{-1}$ harmonic frequency and 2.3 $cm^{-1}$ Ru 100−104 shift, which is not in agreement with the observed band spacings. In addition, the infrared intensity for RuS is much less than for the above antisymmetric stretching modes. Hence, we believe that RuS is not observed in these experiments.

**OsS.** Our DFT calculation finds low $^5\Sigma^+$ and $^5\Delta$ states for OsS with 509 and 494 $cm^{-1}$ harmonic frequencies and 1.0261 sulfur 32/34 isotopic frequency ratios. These are very approximate predictions of the heavy metal OsS vibrational fundamental. A weak 492.4 $cm^{-1}$ band in these experiments sharpens on UV photolysis and shifts to 479.9 $cm^{-1}$ with sulfur-34 (ratio 1.0260). Accordingly, this weak band is appropriate for OsS, which merits a tentative assignment.

**$OsS_2$ and $Os(S_2)$.** The osmium and sulfur product spectrum is complicated as four absorptions with different sulfur isotopic shifts fall in the upper region. The global minimum energy species is open $OsS_2$ in the $^3B_1$ ground electronic state, as found for $RuS_2$, but in the $OsS_2$ case the $^5B_2$ state is now 11 kcal/mol higher in energy. Our best calculation finds the $^3A_2$ ground state of cyclic $Os(S_2)$ to be 44 kcal/mol higher energy than the global minimum energy open species. The first band to notice is the sharp 546.9 $cm^{-1}$ peak, which shifts to 531.2 $cm^{-1}$ with sulfur-34 and defines the large (1.0296) sulfur 32/34 isotopic frequency ratio characteristic of an almost pure S−S stretching mode. The single sharp mixed isotopic counterpart at 539.1 $cm^{-1}$ is precisely at the median of pure isotopic counterparts, as expected for the $Os(S_2)$ molecule without nearby interacting vibrational modes.B3LYP calculation predicts the S−S stretching mode for this molecule at 546.0 $cm^{-1}$, very close to the observed band. The $OsS_2$ molecule unfortunately shares the 537 $cm^{-1}$ band profile with natural isotopic sulfur, but the two bands are resolved with sulfur-34 at 524.9 and 522.6 $cm^{-1}$, and the shoulder at 537.5 $cm^{-1}$ defines the sulfur-32 counterpart and the 1.0240 isotopic frequency ratio. Our calculation for the $^3B_1$ ground electronic state molecule indicates substantial interaction between both stretching modes in the 32-Os-34 isotopic molecule, but these bands are not resolved from other product absorptions in the mixed isotopic spectrum. Thus, the identification of the $OsS_2$ molecule rests on the unique sulfur 32/34 isotopic ratio, which is calculated as 1.0241 and observed as 1.0240.

Although the cyclic $Os(S)_2$ molecule or complex appears to increase on annealing, apparently the more stable $OsS_2$ molecule does not, which suggests that its formation may require activation energy. It is also suggested that $OsS_2$ combines with $S_2$ on annealing to form both $(S_2)OsS_2$ and $OsS_4$. Ultraviolet irradiation clearly favors the final, most stable $OsS_4$ product.

$$Os + S_2 \rightarrow Os(S_2) \quad (1)$$

$$Os + S_2 \rightarrow OsS_2 \quad (2)$$

$$OsS_2 + S_2 \rightarrow (S)_2OsS_2 \rightarrow OsS_4 \quad (3)$$

**$(S_2)OsS_2$.** Three bands at 545.1, 536.8, and 520.2 $cm^{-1}$ track together on annealing and exhibit different sulfur 32/34 isotopic ratios. All three of these bands exhibit asymmetric mixed isotopic triplets with the higher two showing the most coupling between the two modes of the $OsS_2$ functional group when the symmetry is reduced and the lower mode revealing characteristic behavior for an $Os(S_2)$ group. The three bands are calculated at 545.3, 537.4, and 523.0 $cm^{-1}$ for the nonplanar $C_{2v}$ $(S_2)OsS_2$ complex in the $^1A_1$ ground state with sulfur 32/34 isotopic frequency ratios 1.0242, 1.0275, and 1.0301, which are in extremely good agreement with the observed values (Table 1). Even more impressive is the calculation of the mixed isotopic triplets: one S-34 in the $OsS_2$ functional group is predicted to give intermediate components 2.7 and 10.9 $cm^{-1}$ below the all-S-32 values and we observed these bands 2.0 and 10.4 $cm^{-1}$ below, and one S-34 in the $Os(S_2)$ group is predicted to give a mixed component 7.6 $cm^{-1}$ below the all-S-32 value and this band appears 6.5 $cm^{-1}$ lower. In summary, the observation of the three strongest stretching modes and their detailed sulfur-34 substitution character in excellent agreement with B3LYP calculated values confirms the identification of the $(S_2)OsS_2$ complex in the $^1A_1$ ground state.

**$OsS_4$.** The anticipated tetrahedral $OsS_4$ molecule is 3 kcal/mol lower in energy than the above $(S_2)OsS_2$ complex. The same calculation that predicted the above complex fundamentals within 3 $cm^{-1}$ gave the intense triply degenerate mode of $OsS_4$ at 499.4 $cm^{-1}$ with sulfur isotopic frequency ratio 1.0246, and the large Gaussian basis increased this to 500.5 $cm^{-1}$. Our computation of tetrahedral $OsS_4$ is in excellent agreement with a previous theoretical report.[44] This calculation was repeated for all possible mixed sulfur isotopes, and most of the intensity remains in the pure isotopic bands as there is little mode coupling thought the heavy Os metal center, just as observed for $OsO_4$.[27] Weak mixed isotopic bands are predicted 1.2, 2.6, and 4.6 $cm^{-1}$ above the all-34 peak.

The strong 503.7 $cm^{-1}$ band increases on annealing and UV irradiation and shifts to 491.6 $cm^{-1}$ using sulfur-34 with the same frequency ratio as calculated for $OsS_4$. Broadening of the sulfur-34 component in the mixed isotopic experiment is ascribed to the first of the mixed isotopic bands computed for $Os^{32}S_3{}^{34}S$. The chemical behavior of these absorptions is appropriate for their assignment to the stable $OsS_4$ molecule, which is confirmed by the frequency and isotopic shift calcula-

tions. Although $OsO_4$ is a well-known molecule of tetrahedral symmetry,[45,46] we believe that this is the first experimental observation of $OsS_4$.

**Structure and Bonding Trends within the Group 8 Family.** First, let us compare the group 8 disulfide and dioxide molecules, which have all been observed in solid argon matrices. Our DFT calculations showed that the $^3B_1$ and $^5B_2$ states for $FeO_2$ are close in energy, but the observed 945.8 and 797.1 $cm^{-1}$ stretching frequencies and oxygen 16/18 isotopic ratios clearly fit predictions for the $^3B_1$ and not the $^5B_2$ state.[26] The reverse situation holds for $FeS_2$ where the 540.2 and 467.2 $cm^{-1}$ absorptions and sulfur 32/34 isotopic data match the calculations for the $^5B_2$ state and not the higher energy $^3B_1$ state (Table 2). Both $FeO_2^-$ and $FeS_2^-$ were observed in low laser energy experiments where electron capture products are favored.[42c]

The bent $RuO_2$ molecule was well described by isotopic frequencies and calculations for the $^1A_1$ ground electronic state,[27] and the case for the $^3B_1$ ground state of $RuS_2$ has been made in this work. Both $OsO_2$ and $OsS_2$ were adequately described by isotopic frequencies and calculations for the $^3B_1$ ground electronic state. In the case of Fe and Ru, the disulfide has higher spin multiplicity than the dioxide.

The open $MS_2$ disulfide is more stable than the side-bonded $M(S_2)$ complex, and this difference increases with group 8 metal size.

The side-bonded $(\eta^2\text{-}O_2)FeO_2$ complex has been characterized,[26] but the sulfur analog $Fe(S_2)_2$ has both disulfur molecules side-bonded. There is no evidence for the higher energy $FeO_4$ or $FeS_4$ molecules. Both $RuO_4$ and the higher energy side-bonded $(\eta^2\text{-}O_2)RuO_2$ complex were observed,[27] but the lower energy $(\eta^2\text{-}S_2)RuS_2$ complex clearly dominated the $RuS_4$ molecule in the present experiments. In the osmium case, the much lower energy $OsO_4$ molecule exceeded the $(\eta^2\text{-}O_2)OsO_2$ complex band absorbance by more than an order of magnitude whereas $OsS_4$ is only slightly lower in energy than the $(\eta^2\text{-}S_2)OsS_2$ complex, and both species are clearly observed here. These observations are in line with the increasing stability of the VIII oxidation state on going down the group 8 metal family.

## Conclusions

Laser-ablated Fe, Ru, and Os atoms were reacted with small sulfur molecules from a microwave discharge in argon and condensed at 7 K. Numerous reaction products were identified from matrix infrared spectra, sulfur-34 isotopic shifts, spectra of sulfur isotopic mixtures, and frequencies from density functional calculations. The strongest absorptions of the $MS_2$ disulfide molecules are observed at 540.2, 535.5, and 537.5 $cm^{-1}$, respectively, for the group 8 metals. The photosensitive $FeS_2^-$ anion was detected at 542.1 $cm^{-1}$. The $RuS_2$ absorption exhibited five resolved natural ruthenium isotopic splittings. Evidence is also presented for side-bound $M(S_2)$ isomers and $MS_4$ molecules with the structures $Fe(S_2)_2$, $(S_2)RuS_2$, and tetrahedral $OsS_4$, which were computed to be the lowest energy species for this stoichiometry.

**Acknowledgment.** We gratefully acknowledge financial support from NSF Grant CHE 00-78836 and NCSA computing Grant No. CHE07-0004N to L.A.

## References and Notes

(1) Stiefel, E. I., Matsumoto, K., Eds.; *Transition Metal Sulfur Chemistry, Biological and Industrial Significance*; American Chemical Society: Washington, DC, 1997.

(2) Rickard, D.; Luther, G. W., III *Chem. Rev* **2007**, *107*, 514.

(3) Wells, A. F. *Structural Inorganic Chemistry*, 4th ed.; Clarendon: Oxford, UK, 1975. (b) Sourisseau, C.; Cavagnat, R.; Fouassier, M. *J. Phys. Chem. Solids* **1991**, *52*, 537.

(4) (a) Williams, R. J. P. *Nature (London)* **1990**, *343*, 213. (b) Drobner, E.; Huber, H.; Wächtershäuser, G.; Rose, D.; Stetter, K. O. *Nature (London)* **1990**, *346*, 742.

(5) Posfai, M.; Buseck, P. R.; Bazylinski, D. A.; Frankel, R. B. *Science* **1998**, *280*, 880.

(6) McKay, D. S.; Gibson, E. K.; ThomasKeprta, K. L.; Vali, H.; Romanek, C. S.; Clemett, S. J.; Chilier, X. D. F.; Maechling, C. R.; Zare, R. N. *Science* **1996**, *273*, 924.

(7) Cosper, N. J.; Booker, S. J.; Ruzicka, F.; Frey, P. A.; Scott, R. A. *Biochemistry,* **2000**, *39*, 15668.

(8) Ugulava, N. B.; Carlos, J. S.; Jarrett, J. T. *Biochemistry* **2001**, *40*, 8352.

(9) Anxolabehere-Mallart, E.; Glaser, T.; Frank, P.; Aliverti, A.; Zanetti, G.; Hedman, B.; Hodgson, K. O.; Solomon, E. I. *J. Am. Chem. Soc.* **2001**, *123*, 5444.

(10) Frenchard, F.; Sautet, P. *J. Catal.* **1997**, *170*, 402.

(11) Jeevanandam, P.; Koltypin, Y.; Gofer, Y.; Diamant, Y.; Gedanken, A. *J. Mater. Chem.* **2000**, *10*, 2769.

(12) Eckermann, A.; Fenske, D.; Rauchfuss, T. B. *Inorg. Chem.* **2001**, *40*, 1459.

(13) Lassiter, J. C.; Luhr, J. F. *Geochem. Geophys. Geosys.* **2001**, *2*, U1.

(14) MacMahon, T. J.; Jackson, T. C.; Freiser, B. S. *J. Am. Chem. Soc.* **1989**, *111*, 421.

(15) Zhang, N.; Hayase, T.; Kawamata, H.; Nakao, K.; Nakajima, A.; Kaya, K. *J. Chem. Phys.* **1996**, *104*, 3413.

(16) Zhai, H. J.; Kiran, B.; Wang, L.-S. *J. Phys. Chem.* **2003**, *107*, 2821.

(17) Harvey, J. N.; Heinemann, C.; Fiedler, A.; Schröder, D.; Schwartz, H. *Chem.—Eur. J.* **1996**, *2*, 1230.

(18) Schröder, D.; Kretzschmar, I.; Schwartz, H.; Rue, C.; Armentrout, P. B. *Inorg. Chem.* **1999**, *38*, 3474.

(19) Husband, J.; Aguirre, F.; Thompson, C. J.; Metz, R. B. *Chem. Phys. Lett.* **2001**, *342*, 75.

(20) DeVore, T. C.; Franzen, H. F. *High Temp. Sci.* **1975**, *7*, 220. The 542 $cm^{-1}$ Fe and OCS reaction product first assigned to FeS is due to another species.

(21) Takano, S.; Yamamoto, S.; Saito, S. *J. Mol. Spectrosc.* **2004**, *224*, 137.

(22) Bauschlicher, C. W. Jr.; Maitre, P. *Theor. Chim. Acta* **1995**, *90*, 189.

(23) (a) Hübner, O.; Termath, V.; Berning, A.; Sauer, J. *Chem. Phys. Lett.* **1998**, *294*, 37. (b) Hübner, O.; Sauer, J. *Phys. Chem. Chem. Phys. Lett.* **2002**, *4*, 5234.

(24) (a) Bridgeman,A. J.; Rothery, J. *J. Chem. Soc., Dalton Trans.* **2000**, *211*. (b) Mebel, A. M.; Hwang, D.-Y. *J. Phys. Chem. A* **2001**, *105*, 7460.

(25) Clima, S.; Hendrickx, M. F. A. *Chem. Phys. Lett.* **2007**, *436*, 341.

(26) (a) Andrews, L.; Chertihin, G V.; Ricca, A.; Bauschlicher, C. W., Jr. *J. Am. Chem. Soc.* **1996**, *118*, 467. (b) Chertihin, G. V.; Saffel, W.; Yustein, J. T.; Andrews, L.; Neurock, M.; Ricca, A.; Bauschlicher, C. W. Jr. *J. Phys. Chem.* **1996**, *100*, 5261. (c) Gong, Y.; Zhou, M.; Andrews, L., *J. Phys. Chem. A* **2007**, *111*, 12001 (Fe + $O_2$).

(27) Zhou, M.; Citra, A.; Liang, B.; Andrews, L. *J. Phys. Chem. A* **2000**, *104*, 3457.

(28) Liang, B.; Andrews, L. *J. Phys. Chem. A* **2002**, *106*, 3738.

(29) Liang, B.; Andrews, L. *J. Phys. Chem. A* **2002**, *106*, 6295.

(30) Brabson, G. D.; Mielke, Z.; Andrews, L. *J. Phys. Chem.* **1991**, *95*, 79.

(31) (a) Andrews, L.; Citra, A. *Chem. Rev.* **2002**, *102*, 885. (b) Andrews, L.; Cho, H.-G. *Organometallics* **2006**, *25*, 4040.

(32) Cho, H.-G.; Lyon, J. T.; Andrews, L. *Organometallics* **2008**, *27*, 5241.

(33) Frisch, M. J.; et al. *Gaussian 98, revision A.1*; Gaussian, Inc.: Pittsburgh, PA, 1998.

(34) (a) Becke, A. D. *J. Chem. Phys.* **1993**, *98*, 5648. (b) Lee, C.; Yang, Y.; Parr, R. G. *Phys. Rev. B* **1988**, *37*, 785.

(35) Perdew, J. P.; Wang, Y. *Phys. Rev. B* **1992**, *45*, 13244.

(36) Raghavachari, K.; Trucks, G. W. *J. Chem. Phys.* **1989**, *91*, 1062.

(37) Hay, P. J.; Wadt, W. R. *J. Chem. Phys.* **1985**, *82*, 270. (a) Wadt, W. R.; Hay, P. J. *J. Chem. Phys.* **1985**, *82*, 284. (b) Hay, P. J.; Wadt, W. R. *J. Chem. Phys.* **1985**, *82*, 299.

(38) Frisch, M. J.; et al. *Gaussian 03, Revision C.02*; Gaussian, Inc.: Pittsburgh, PA, 2003.

(39) Andrae, D.; Haeussermann, U.; Dolg, M.; Stoll, H.; Preuss, H. *Theor. Chim. Acta* **1990**, *77*, 123.

(40) (a) Long, S. R.; Pimentel, G. C. *J. Chem. Phys.* **1977**, *66*, 2219. (b) Smardzewski, R. R. *J. Chem. Phys.* **1978**, *68*, 2878.

(41) The natural abundances of $^{102}$Ru and $^{104}$Ru are 32% and 19%. *CRC Handbook of Chemistry and Physics*; CRC Press: Boca Raton, FL, 1985.
(42) (a) Zhou, M.; Andrews, L. *J. Am. Chem. Soc.* **1998**, *120*, 11499. (b) Zhou, M.; Andrews, L.; Bauschlicher, C. W., Jr. *Chem. Rev* **2001**, *101*, 1931. (c) Li, Z. H.; Gong, Y.; Fan, K.; Zhou, M. *J. Phys. Chem. A* **2008**, *112*, 13641.
(43) Liang, B.; Wang, X.; Andrews, L. *J. Phys. Chem. A* **2009**, *113*, in press (Ni, Pd, Pt + $S_2$).
(44) Zli, S.; Stoll, H.; Baerends, E. J.; Kaim, W. *Inorg. Chem.* **1999**, *38*, 6101.
(45) McDowell, R. S.; Goldblatt, M. *Inorg. Chem.* **1971**, *10*, 625.
(46) Cotton, F. A.; Wilkinson, G.; Murillo, C. A.; Bochmann, M. *Advanced Inorganic Chemistry*, 6th ed.; Wiley: New York, 1999.

JP900994C